Prediction of Central Recirculation Zone Size for a Complete Burner-Quarl-Furnace System

Eugen-Dan B. Cristea*
Institute of Scientific Research and Engineering for Power Equipment, Bucharest, Romania

In the swirl flow burning process of fuels, the central recirculation zone plays an important role in flame stabilization by providing a hot flow of recirculated combustion products, which reduce both the length of flame and the stabilized flame distance from the burner mouth. In this paper, a new modified swirl number, S^{xx}, related to the characteristic size of the burner quarl, is introduced to correlate the isothermal and burning flows. Using a well-known two-dimensional computational model, the isothermal flow pattern in a complete burner-quarl-furnace system is computed. On this basis, the theoretical swirl number S^{xx} is calculated and used as a correlation parameter for predicting the central recirculation zone size in burning flow conditions. Experimental tests for both nonreacting and reacting flows on the same complete burner-quarl-furnace system, for comparing the theoretical and experimental swirl number S^{xx}, have been conducted, and the validity of this new correlation parameter has been proved.

Nomenclature

B	= burning conditions
C_η	= coefficient in Eq.(2)
d	= diameter, m
G_x	= axial flux of the linear momentum, N
G_Φ	= axial flux of the angular momentum, Nm
I	= isothermal conditions
k	= kinetic energy of turbulence, m^2/s^2
ℓ	= quarl length, m
$\mathring{M}$	= mass flow rate, kg/s
p	= pressure, N/m^2
r	= radial coordinate, m
S, S^x, S^{xx}	= swirl number expressions
S_Φ	= source term for the Φ fluid property, ... kg/m^3s
v_x, v_r, v_ϑ	= velocity components in the cylindrical polar system of coordinates, m/s
W	= time-averaged square of the vorticity fluctuations, $(1/s^2)$
x	= axial coordinate, m
α	= half-angle of burner quarl, deg
β	= angular overlap of vane, deg
γ	= vane angle to the axial direction, deg
Γ_Φ	= turbulent exchange coefficient, kg/ms
δ	= width of annular swirler support, m
η	= dynamic viscosity, kg/ms
ν	= kinematic viscosity, m^2/s
ρ	= density, kg/m^3
σ_Φ	= effective Prandtl–Schmidt's number
Φ	= general fluid property (dependent variable)
Ψ	= stream function, kg/s
ω	= vorticity, 1/s
ϑ	= polar coordinate, deg

Superscripts

M	= maximum
T	= total
$\bar{(\ )}$	= time-averaged
$\hat{(\ )}$	= angle

Subscripts

a	= air
b	= burner mouth
c	= characteristic
d	= dynamic
e	= experimental
eff	= effective
F	= fuel
f	= furnace
q	= quarl
r	= recirculate
ref	= reference
s	= static
te	= theoretical
0	= input (initial)

Received Jan. 28, 1985; revision received June 12, 1986.

*Head, Laboratory-Research Department.

Introduction

DURING the last decades, concentrated research efforts have been expended on understanding and characterizing the combustion aerodynamics of the swirl flow burning processes, with particular regard to the main effects of swirl on the performance, stability, and combustion intensity of industrial flames.[1] The flame stabilization is governed by many factors, such as burner and quarl geometry, furnace dimensions, air and fuel stream velocities, turbulence levels, etc. In diffusion flames, separate streams of air and fuel enter the furnace, and the burning process is controlled mainly by the mixing rate of the two reactants. This work combines experimental and theoretical combustion aerodynamics with sophisticated computational fluid dynamics for predicting the flow pattern in a complete burner-quarl-furnace system, using a new modelling parameter.

The traditional "cut-and-try" methods of designing the complete burner-quarl-furnace system with a stabilized flame with maximum combustion efficiency and minimum pollutant emission have become increasingly expensive and time consuming. The ability of the mathematical methods to predict quickly and economically the burning process in different geometries of the complete burning systems commends the same to the combustion engineers. This theoretical approach may also provide guidance as to the ways in which a design should be improved to considerably reduce the experimental test program required to achieve a good design.

The mathematical model of two-dimensional, nonreacting, swirling, recirculating, turbulent flows simulates the aerodynamics inside a complete isothermal burner-quarl-furnace system by means of differential equations for the dependent variables. The governing well-established conservation equations of mass and momentum are added with the turbulent model necessary to solve the equation set. The simultaneous solution of all of these equations, solved by a finite difference procedure, yields the values of the dependent variables at all grid nodes that cover the flowfield. The results of this theoretical investigation have been summarized in Ref. 2.

The primary purpose of the present work is to introduce a new modified swirl number, S^{xx}, related to the quarl characteristic size for predicting the flow pattern in a low-pressure auxiliary fluid spray burner-divergent quarl-cylindrical furnace system.

Based on the computer program, the cross-transversal distribution of axial, tangential and radial velocities in various isothermal flowfield sections and the theoretical swirl number S^{xx} were computed. Experimental trials were performed on the plexiglass rig and on industrial facility, in burning conditions, on which trials the velocity profiles in the same sections were measured and the experimental swirl number S^{xx} was computed. The compared isothermal and burning tests showed that the shape and size of the central recirculation zone (CRZ) were primarily a quarl geometry function. The swirl number S^{xx} can be used as a modelling parameter of the flowfield and to predict CRZ types, as it was found that the velocity profiles downstream of the maximum CRZ diameter are similar at the same S^{xx} value for the same flowfield section.

It is the author's desire, that the results presented herein will be of the same interest and value to the combustion engineers.

Experimental Details

Figure 1 shows the experimental facility scheme with the cylindrical furnace uncooled refractory brick-wall type of 0.600-m i.d. and 1.3-m long having all of the necessary supplies. The front wall supports a coaxial burner and, on both sides of the equatorial plane of the walls there are eight ports for measuring the flame characteristics. An identical isothermal plastic furnace was used for the tests in nonburning conditions.

The burner used was one with low-pressure auxiliary fluid spray, named ACLU-500, in which the spray momentum is small as compared to the airflow momentum.[3] In this case, the characteristic dimensions of the flame depend more on the airflow pattern than on the fuel spray.[4,5] The burner of

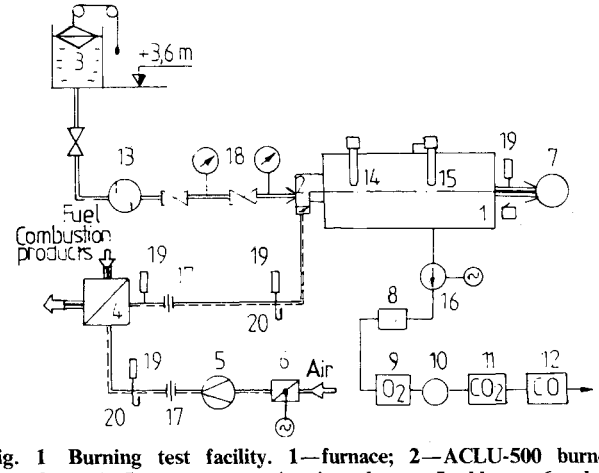

Fig. 1 Burning test facility. 1—furnace; 2—ACLU-500 burner; 3—volumetric flow rate meter; 4—air preheater; 5—blower; 6—clock valve; 7—chimney; 8—drayer; 9—oxygen analyzer; 10—flowmeter; 11-12—infrared analyzers; 13—filter; 14—five-hole probe; 15—probe; 16—sample electropump; 17—orifice meter; 18—manometers; 19—thermometers; 20—U manometers; 21—micromanometer.

0.5MW$_t$ input thermal power contains two air circuits, both having swirl generator systems. The primary air circuit includes a tangential entry swirl generator, and the secondary one includes an annular vane swirl generator. Coaxial with the swirl generators there is a fuel pipe with a Venturi-shape nozzle. Thirteen types of annular flat vane swirlers (AFVS) $\hat{\gamma}/\hat{\beta}$ (δ) and 12 types of annular spin vane swirlers (ASVS) $\hat{\gamma}/\hat{\beta}$ (δ) of 0.126-m o.d. and 0.086-m i.d. were used. The swirlers include 12 vanes forming 15; 30; 45 and 60-deg angles to the burner axis, in two construction types with the constant angular overlap of vane ($\hat{\beta} = 30$ deg) and the constant width of annular swirler support ($\delta = 30$ mm), respectively. Two quarl types of expansion ratios, $d_q/d_b = 2$ and 3.5, and 0.260-m constant length and 0.090-m constant inlet diameter were used for both isothermal and burning tests.

In addition to the ordinary measurements of flow rates, temperatures, pressures on fuel, and air combustion circuits, the radial velocity distributions were measured by means of a five-hole cooled probe for burning conditions and five-hole uncooled probe (the "Instruments de presion MDG-EDF" French type) plus hot-wire anemometer DISA—Denmark for isothermal conditions. The temperature profiles were measured by a small-dimension Pt-Rh-Pt aspirator thermocouple, and the resulting electromotive force was read directly on a digital voltmeter with cold junction compensation.

The experimental burning conditions adopted are tabulated in Table 1. The nominal burner operation regime (No. 1) was fully tested from an aerodynamics viewpoint, using the same physical parameters in both burning and nonburning conditions.

The quarl-furnace flowfield was investigated, taking into account the few parameters influencing the pattern model: quarl semiangle, burner mouth and furnace radii ratio, Reynolds number, and swirl number. Two parameters were permanently fixed: $r_b/r_f = 0.15$ and $Re = 1.51 \times 10^5$ and, in addition, the quarl semiangle had two constant values ($d_q/d_b = 2$ and 3.5 for $\ell_q = ct$ and $d_b = ct$). The inlet conditions of the flowfield were modified by swirl number variation, using different types of annular vane swirlers. The fuel used for burning conditions was light fuel oil whose properties are listed in the Appendix.

Governing Equation System for Isothermal Conditions

The turbulence Reynolds equations of conservation of mass, momentum (in the x, r, and ϑ directions), turbulent energy k, and square of the vorticity fluctuations W, which govern the two-dimensional axisymmetric, isothermal, turbulent, swirling, steady flow, may be taken as in previous works.[6-8] The transport equations are all similar and contain terms for the convection, diffusion, and source of a general variable, Φ.

The general form of the balance equation for a general fluid property Φ is expressed as

$$\frac{1}{r}\left\{\frac{\partial}{\partial r}(\rho r \bar{v}_r \Phi)\right\} + \frac{\partial}{\partial x}(\rho \bar{v}_x \Phi) - \frac{1}{r}\left\{\frac{\partial}{\partial r}\left(r\Gamma_\Phi \frac{\partial \Phi}{\partial r}\right)\right\} - \frac{\partial}{\partial x}\left(\Gamma_\Phi \frac{\partial \Phi}{\partial x}\right) - S_\Phi = 0 \tag{1}$$

for $\Phi = 1$ (continuity equation); $\bar{v}_x$, $\bar{v}_r$, $\bar{v}_\vartheta$ are three velocity components and k and W (are two turbulence quantities). The source term S_Φ contains terms describing the generation and dissipation of Φ; their forms are given in Ref. 7. The turbulence model applied is a two-equation model, namely, k-W, and the local effective eddy viscosity and turbulent exchange coefficient may be expressed as

$$\eta_{\text{eff}} = C_\eta \rho k/\sqrt{W}, \quad \Gamma_\Phi = \eta_{\text{eff}}/\sigma_\Phi \tag{2}$$

The work is based on the stream function-vorticity ($\Psi - \omega_\vartheta$) formulation of the equation system, which must be solved for

Table 1 Experimental conditions

Item	Regime 1	Regime 2	Regime 3	Regime 4
Input thermal power, MW_t	0.475	0.370	0.233	0.156
Fuel flow rate, kg/s	0.0114	0.0089	0.0056	0.0038
Fuel pressure, daN/m^2				
Upstream	2430	2432	2435	2437
Downstream	1750	1160	690	480
Fuel temperature, K	302	302	302	302
Total airflow rate, kg/s	0.1718	0.1370	0.0703	0.0498
Aerodynamic burner resistance, daN/m^2 (at temperature 305 K)	475	310	150	100
Average combustion, CO_2	15	14.4	13.8	13.2
Product composition, O_2	1.2	2.0	2.8	3.6
Vol.%, CO	0	0	0	0
Bacharach smoke index	0	0	1	1
Air excess	1.06	1.1	1.15	1.2
Pressure in furnace, daN/m^2	−3.0	−2.0	−2.0	−1.0
Flame length, m	1.1	0.9	0.7	0.6
Noise level, dB	95/83	—	—	—

the time-averaged dependent variables Ψ, ω_ϑ/r, rv_ϑ, k, and W.

The elliptical, nonlinear, second-order, partial differential equation system was simultaneously solved using the digital method on the finite difference technique. The recurrence formula (cf. Ref. 6) is used to solve simultaneously for the Φ-dependent variables in each of the grid nodes by means of the point-by-point Gauss-Seidel method. Special treatment of the corner singularities and inclined quarl walls was achieved.[9] With a computer program, a maximum 30×30 nonuniform, orthogonal grid was produced and the run time (on an IBM 360/40 computer) with an iteration of 6 s/node was achieved.[8,9]

New Modified Swirl Number S^{xx}

The swirling jets result from the application of a spiraling motion on the fluid stream, which is imparted to the flow via swirlers such as swirl vanes, tangential entry, rotary pipes, etc.

Chigier and Béer[10] characterized the degree of swirl by the swirl number S, which is a nondimensional number expressed as

$$S = \left(\int_0^\infty v_x v_\vartheta r^2 \mathrm{d}r\right) \Big/ \left\{ r_c \int_0^\infty \left[\rho v_x^2 + (p - p_{\text{ref}})\right] r \mathrm{d}r \right\} \quad (3)$$

Unfortunately, this definition did not completely characterize the swirl jets, as the flow after the swirl generator exit depends on other factors, such as quarl dimensions and effect of the enclosing walls.

Beltagui and Maccallum[11] have studied the premixed vane swirled flames in furnaces, without quarl, with furnace burner expansion ratios $d_f/d_b = 2.5$ and 5. They found that the same swirler can give different velocity patterns as the relative furnace size d_f/d_b is changed. At the same time, the size and shape of the CRZ is primarily dependent on furnace diameter and not on swirl vane diameter. Beltagui and Macallum proposed a modified swirl number expressed as follows:

$$S^x = G_\Phi / \left(G_{x_d} d_f\right) \quad (4)$$

The analysis of flow pattern models occurring inside the complete burner-quarl-furnace system is necessary for noting the important role played by the quarl in flame stabilization. This role is well known to combustion engineers, but there is a need for a theoretical-experimental scientific demonstration considering the following:

1) The radial distribution of the velocity vector components and the pressure at the swirl generator exit are nonuniform (due to construction and mounting).

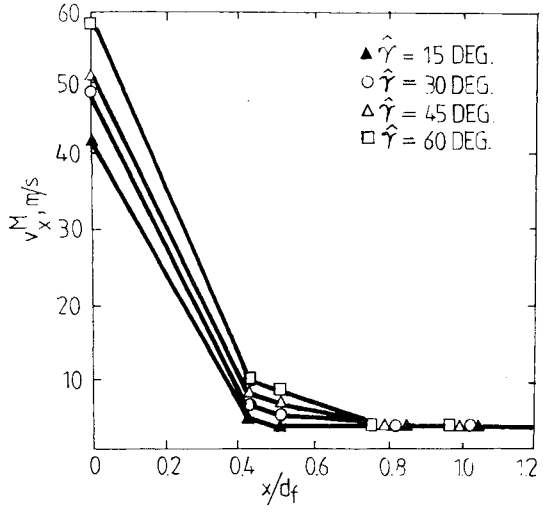

Fig. 2 Maximum axial velocity variations on axial direction for $d_q/d_b = 2$ (ASVS $\hat{\gamma}/\hat{\beta}$).

2) The same burner, equipped with a combination tangential entry and annular vane swirler, in the same furnace, can produce different radial distributions of velocity vector components when the quarl geometry is changed (the expansion ratios are $d_q/d_b = 2$ and 3.5).

3) Experimental tests on the model and prototype revealed that the shape and size of the CRZ are primarily functions of the quarl geometry and not of the swirl generator diameter.

For these reasons, a new modified swirl number was proposed by the present author in Ref. 9.

$$S^{xx} = G_\Phi / \left(G_{x_d} r_q\right)$$

where

$$r_q = f(\hat{\alpha}) \quad \text{for} \quad \ell_q = ct,\ d_b = ct \quad (5)$$

For the analysis of a flow pattern in isothermal or burning conditions, it was necessary to take into account four flow types:

1) Type I, which has the maximum axial velocity located on the axis of the burner-quarl-furnace, is typical for very weak swirl and unswirled flows.

2) In type II, there are few differences from the first type but, in this case, the radial distribution of axial velocity has two small maxima near the wall, without a CRZ.

3) Type III shows a reduced CRZ on the axis.

4) Type IV is characterized by a strongly established CRZ. For a good delimitation between this flow type and types I–III, an arbitrary value was chosen at the ratio $\dot{M}_r/\dot{M}_0^T = 0.330$, which was obtained for a vane angle of swirl vanes of 45 and 60 deg in isothermal and burning conditions.

The transition between these types, in isothermal and burning conditions for a given burner, furnace, and given air-fuel ratio, occurs at new modified swirl number S^{xx} values, which are very similar for the two relative quarl sizes.

Discussion of the Results

The very large volume of experimental data on the model and prototype and the computed results for the model in Ref. 9 permit a comparison, and the conclusions are presented here. The main data are tabulated in Table 2 and analyzed as follows:

1) The maximum relative diameter of the CRZ, d^M_{CRZ}/d_q, is not visibly influenced by the swirl number increase after a well-stabilized CRZ; its value has been determined by the quarl semiangle, i.e., the hydraulic outlet quarl diameter d_q ($\ell_q = ct$, $d_b = ct$). On the other hand, d^M_{CRZ} is little influenced by the d_q/d_b increase, and the burning process has a very slight effect upon d^M_{CRZ}/d_q in the case of the big quarl.

2) The relative length of the CRZ, ℓ_{CRZ}/d_q, is greatly affected by the swirl number variation; a small decrease was recorded as a function of the d_q/d_b increase, and the burning conditions did not produce a variation of CRZ length.

3) The nondimensional ratio $v^M_{x_r}/\bar{v}_x$ is strongly dependent of the d_q/d_b variations; the ratio $v^M_{x_r}/\bar{v}_x$ slightly increases with the swirl number increase, but increases very strongly in burning conditions as compared to the isothermal conditions.

4) The theoretical and experimental new modified swirl number S^{xx}, calculated by the axial and tangential radial distribution integration for the experimental and theoretical data, concurred for both quarls.

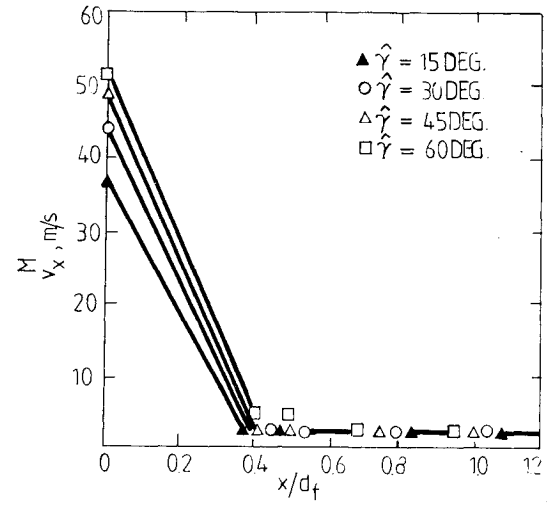

Fig. 3 Maximum axial velocity variations on axial direction for $d_b/d_q = 3.5$ (ASVS $\hat{\gamma}/\hat{\beta}$).

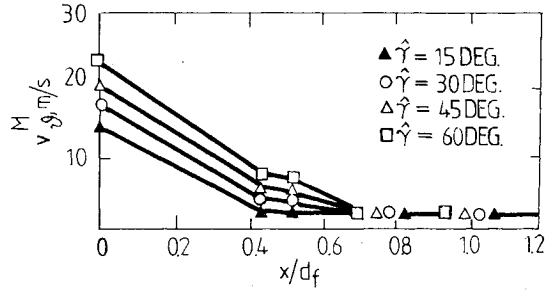

Fig. 4 Maximum tangential velocity variations on axial direction for $d_b/d_q = 2$ (ASVS $\hat{\gamma}/\hat{\beta}$).

Table 2 CRZ characteristics

ASVS $\hat{\gamma}/\hat{\beta}(\delta)$ types	$\frac{d_q}{d_b}$	Flow type	S^{xx}_{te}	S^{xx}_e	$\frac{x}{d_f}$	$\frac{\ell_{CRZ}}{d_f}$	$\frac{d^M_{CRZ}}{d_q}$	$\frac{v^M_{x_r}}{\bar{v}_x}$	$\frac{\dot{M}^M_r}{\dot{M}^T_o}$
I 0/(30)	2	I	0	0		—	—	—	—
15/(30)		II	0.382	0.3931	> 1.016	—	—	—	—
30/30		III	0.425	0.4133		1.55	0.814	0.1208	0.398
30/(30)		III	0.512	0.5323	> 1.016	1.59	0.851	0.1208	0.402
45/30		IV	0.634	0.6406		1.851	0.850	0.116	0.4873
45/(30)		IV	0.705	0.7209	~ 1.15	1.925	0.850	0.150	0.4809
60/30		IV	0.920	0.9226		2.037	0.887	0.158	0.532
60/(30)		IV	0.947	0.9498	1.016	2.11	0.925	0.1375	0.540
B 30/30		III	—	0.418		1.55	0.814	0.587	0.380
30/(30)		III	—	0.5415	> 1.016	1.59	0.851	0.496	0.400
45/30		IV	—	0.6272		1.851	0.850	0.525	0.465
45/(30)		IV	—	0.675	~ 1.15	1.925	0.850	0.6375	0.459
60/30		IV	—	0.8969		2.037	0.887	0.650	0.527
60/(30)		IV	—	0.8872	1.016	2.11	0.925	0.5916	0.511
I 0/(30)	3.5	I	0	0		—	—	—	—
15/(30)		II	0.381	0.3921	> 1.016	—	—	—	—
30/30		III	0.420	0.4140	0.510-760	0.903	0.726	0.040	0.403
30/(30)		III	0.543	0.560		0.945	0.748	0.038	0.421
45/30		IV	0.632	0.6346	0.510-760	1.100	0.748	0.040	0.474
45/(30)		IV	0.738	0.7507		1.144	0.770	0.046	0.476
60/30		IV	0.952	0.9667	0.510-760	1.211	0.748	0.054	0.532
60/(30)		IV	0.987	0.9996		1.254	0.770	0.050	0.533
B 30/30		III	—	0.4124	0.510-760	0.903	0.726	0.154	0.358
30/(30)		IV	—	0.534		0.945	0.748	0.146	0.382
45/30		IV	—	0.6028	0.310-760	1.100	0.748	0.159	0.435
45/(30)		IV	—	0.7475		1.144	0.778	0.208	0.427
60/30		IV	—	0.9147	0.510-760	1.211	0.748	0.208	0.505
60/(30)		IV	—	1.0398		1.254	0.770	0.196	0.478

5) The nondimensional ratio $\mathring{M}_r^M/\mathring{M}_0^T$ increases with the swirl number increase.

The general effect of the burning process as compared to the isothermal conditions was to increase the axial velocity. The increase of the swirl number, using various annular spin vane swirlers of vane angles from 15 to 60 deg, produced an accelerated jet spread and a measure of such a spread in the distance between the jet origin and the point of impact with the furnace walls. At high values of the swirl number, a CRZ characterized by maximum-size diameter and length was located on the symmetry axis. The longitudinal distributions of maximum axial velocities in different sections (inlet quarl, $x/d_f = 0$; outlet quarl, $x/d_f = 0.433$; furnace sections, $x/d_f = 0.766$; 1.016) (Figs. 2 and 3), show the following.

1) Type I flow is characterized by a small, decreasing gradient to the impact point on the furnace wall, thereafter the increase becomes constant.

2) For flow types II and III, the decreasing gradient is higher at the same distance; thereafter, a small decrease continues. The zone where the initial decrease stops is moved toward high x/d_f values in conjunction with the swirl number increase.

3) For type IV flow, the axial velocity decrease is similar to the one in regimes II and III but faster, more uniform, and stopping at the distance $x/d_f = 0.5$.

The main effect of burning conditions as compared to the isothermal conditions was a small increase of tangential velocity.

For flow regimes III and IV, which had a CRZ on the symmetry axis, the maximum tangential velocity position rapidly moved toward the furnace walls. The tangential velocity values in the CRZ and PRZ (peripheral recirculation zone) are small. For flow types I and II, the tangential velocity spread is not so fast, outside of the maximum located near the walls.

The longitudinal distributions of maximum tangential velocities (Figs. 4 and 5), show the following.

1) Flow types I and II had a decrease to an ordinary value, after which the same became constant.

2) Type III flow had the same development: First, an initial fast decrease, then a slow decrease to the constant value was recorded.

The axial flux of the angular momentum computation was made by that axial and tangential radial distribution integration for experimental isothermal and burning conditions (Figs. 6 and 7).

The analysis of the dependence of G_Φ on x/d_f showed that, even if in the first region of the flow pattern, particularly for the case $d_q/d_b = 3.5$, the velocities are small and difficult to measure, downstream from the place where the CRZ gave

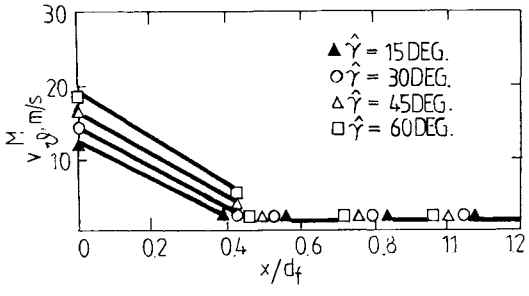

Fig. 5 Maximum tangential velocity variation on axial direction for $d_b/d_q = 3.5$ (ASVS $\hat{\gamma}/\hat{\beta}$).

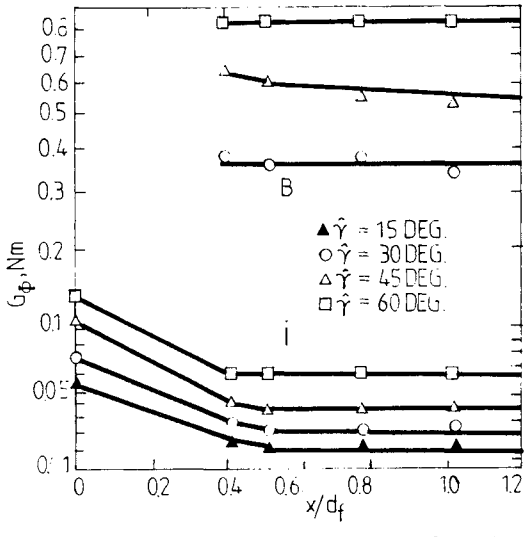

Fig. 6 Axial flux of angular momentum longitudinal distributions for $d_q/d_b = 2$ (ASVS $\hat{\gamma}/\hat{\beta}$).

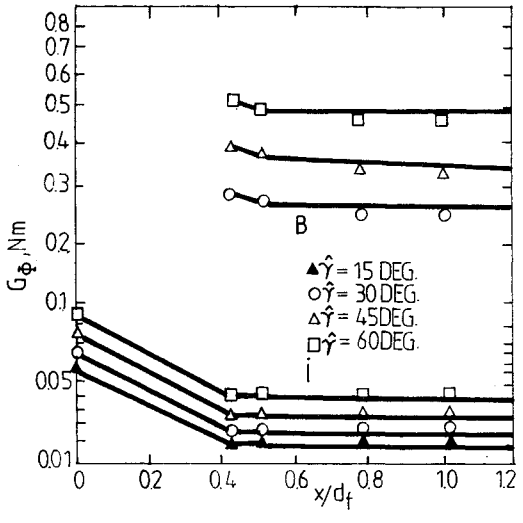

Fig. 7 Axial flux of angular momentum longitudinal distributions for $d_q/d_b = 3.5$ (ASVS $\hat{\gamma}/\hat{\beta}$).

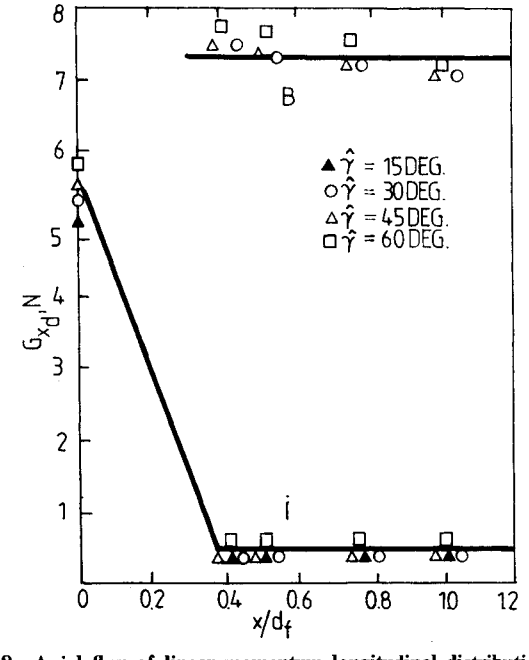

Fig. 8 Axial flux of linear momentum longitudinal distributions for $d_q/d_b = 2$ (ASVS $\hat{\gamma}/\hat{\beta}$).

the maximum diameter, the axial flux of the angular momentum became more uniform.

G_Φ increases with the vane angle increase for both isothermal and burning conditions, for all ASVS types. The maximum values were found at the burner mouth, and larger in the burning conditions than in the isothermal ones.

The axial flux of the linear momentum contains two terms: dynamic and static.

$$G_x = G_{x_d} + G_{x_s} = 2\pi\int_0^\infty \rho v_x r\,dr + 2\pi\int_0^\infty (p - p_{\text{ref}})\,r\,dr \quad (6)$$

The total impulse calculation is difficult because of the reference pressure to be chosen from the possible ones: the atmospheric pressure outside the furnace, the static pressure near the wall, the static pressure inside the CRZ, and the static pressure in the middle of the PRZ. The latter one permits the static term to introduce the swirl and burning effects into the total impulse. However, because the influence of the static impulse term is small, the new modified swirl number definition uses only the dynamic term of the axial flow of the linear momentum.

The dynamic impulse was computed in a similar manner; by the integration of the axial velocity distributions for the experimental isothermal and burning conditions (Figs. 8 and 9).

The analysis of the dependence G_{x_d} vs x/d_f showed that, after the first flow pattern region, where the big fluctuation occurs, the dynamic impulse becomes approximately constant at the nondimensional distances $x/d_f \geq 0.4$.

The dynamic impulse obviously decreases with the ratio d_q/d_b increase; it is bigger in the burning conditions than in the isothermal ones and smaller for bigger d_q/d_b values because of the faster jet expansion, which produces smaller axial velocities.

For the complete burner-quarl-furnace system, it has been shown that the transit among various flow regimes was made at the same S^{xx} value, independently of the d_q/d_b ratio for isothermal and burning conditions. Figure 10 shows that, for the same swirl degree, the new modified swirl number S^{xx} is similar for the two d_q/d_b ratios in isothermal and burning conditions and the curve points are grouped on a straight line. The transition between flow regimes I and II took place at $S^{xx}_{\text{I-II}} = 0.38$, between regimes II and III at $S^{xx}_{\text{II-III}} = 0.41$ and

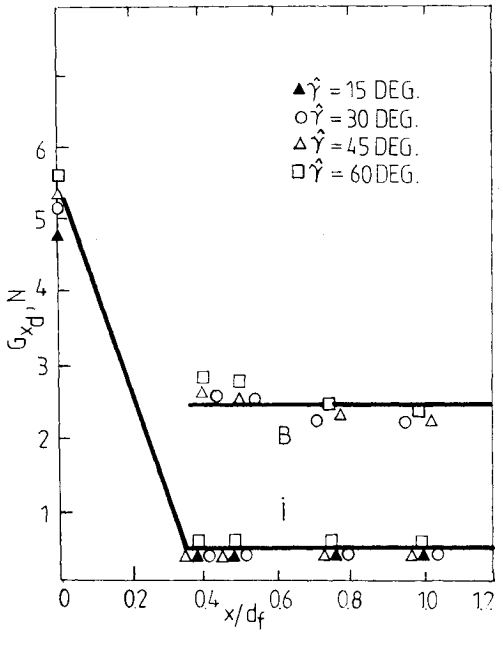

Fig. 9 Axial flux of linear momentum longitudinal distributions for $d_q/d_b = 3.5$ (ASVS $\hat{\gamma}/\hat{\beta}$).

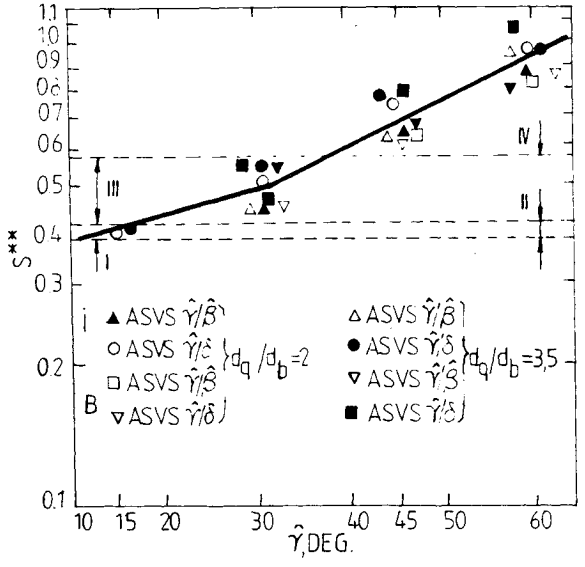

Fig. 10 Dependence of S^{xx} vs vane angle $\hat{\gamma}$.

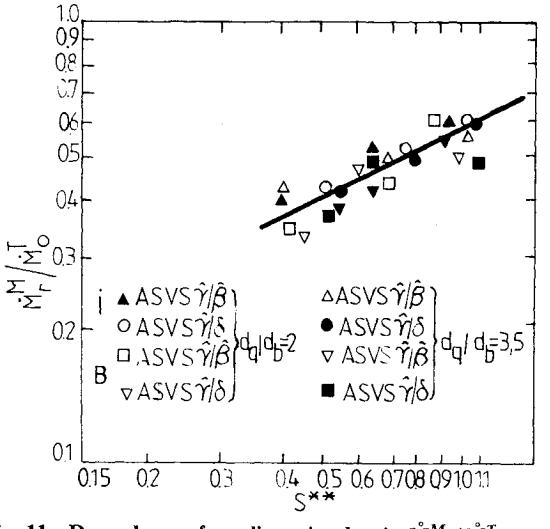

Fig. 11 Dependence of nondimensional ratio $\mathring{M}_r^M/\mathring{M}_o^T$ vs S^{xx}.

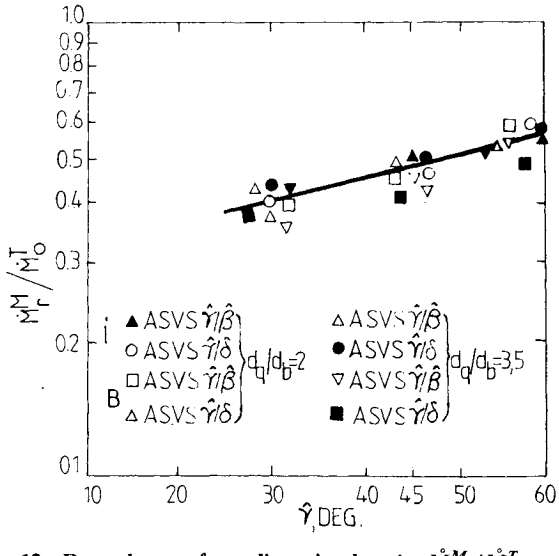

Fig. 12 Dependence of nondimensional ratio $\mathring{M}_r^M/\mathring{M}_o^T$ vs vane angle $\hat{\gamma}$.

for III and IV at $S^{xx}_{III-IV} = 0.59$ in isothermal and burning conditions. The 30-deg vane angle caused the CRZ to settle on the symmetry axis, and a straight line slope modification for the isothermal conditions was recorded.

The new modified swirl number can be used as a modeling parameter of flow patterns and for the prediction of the size and shape of the CRZ, which is located on the symmetry axis inside the quarl and the furnace entrance, as it was found that the velocity profiles downstream of the maximum CRZ diameter were similar at the same x/d_f distances and same S^{xx} values.

In the case of the low-pressure auxiliary fluid spray burner, it was found that the equivalence between the flow pattern in the model and the one in the prototype is possible to attain by the ratio of the maximum recirculating mass flow rate to the total swirler mass flow.

The dependence $\mathring{M}_r^M/\mathring{M}_o^T$ vs S^{xx} and $\mathring{M}_r^M/M_o^T$ vs $\hat{\gamma}$ (Figs. 11 and 12) showed that, for the $d_q/d_b = 2$ and 3.5 ratios, there was a satisfactory correlation of the recirculating mass flow rates in the isothermal and burning conditions and, for the same vane angle, the recirculating flow rate in burning conditions for $d_q/d_b = 3.5$ was similar to the rate in isothermal conditions for the case $d_q/d_b = 2$.

Conclusions

This paper was intended to describe a method in which the isothermal flow in the complete burner-quarl-furnace model was determined by means of a two-dimensional computational model and, on such basis, the burning flow in the prototype was predicted using a new modified swirl number S^{xx}.

It was shown that the transition among various different flow regimes in the complete burner-quarl-furnace system is made at the same new modified swirl number S^{xx} values, independently of the d_q/d_b ratios for isothermal and burning conditions. S^{xx} can be used as a modeling parameter of the flow patterns and for the prediction of the central recirculation zone's (CRZ) size and shape, as it was shown that the velocity profiles downstream of the maximum CRZ diameter are similar at the same x/d_f distances and same S^{xx} value. The equivalence between the flow model in burning and isothermal conditions can be satisfactorily obtained using the ratios of the recirculating mass flow rate to the total mass flow rate.

The application of the method suggested herein was performed on a low-pressure auxiliary fluid spray burner with an annular spin vane swirler generator. As for the design, if the selected vane swirlers are similar to those described in this work, the information presented will provide satisfactory predictions of the flow model and CRZ size and shape. The primary purpose of this paper was to make available to the combustion engineers useful data on the flame stabilization process.

Appendix

The properties of the light fuel oil are as follows:

Chemical analysis: $C = 86.77\%$, $H = 11.75\%$, $S = 0.45\%$, $O = 0.30\%$, others 0.53%

Viscosity: $\nu_{26°C} = 27$ cSt, $\nu_{54°C} = 20$ cSt

Condrason index: 3.12% $H_2O = 0.20\%$

Relative density: $\rho_{25°C} = 0.904$

Calorific value: 41,403 kJ/kg_F

Stoichiometric air-fuel ratio by mass: 14.13 kg_a/kg_F

Acknowledgements

The author sincerely wishes to thank Dr. R. Rosa of the Mechanical Engineering Department of Montana State University for helpful discussions. Many thanks to the International Research Exchange Board for sponsoring the author's stay at Montana State University during the time that this work was crystallized and written.

References

[1] Lilley, D.G., "Swirl Flows in Combustion: A Review," *AIAA Journal*, Vol. 15, Aug. 1977, pp. 1063–1078.

[2] Khalil, E.E., *Modelling of Furnaces and Combustors*, Abacus Press, Tunbridge Wells, Kent, 1982, pp. 13–51.

[3] Lemnean, N., Cristea, E.D., and Jianu, C., *Burning Installations on Liquid Fuels* (in Romanian), Technical Publisher, Bucharest, 1982, pp. 233–234.

[4] Ghiea, V. and Cristea, E.D., "Determination of the Characteristic Curves of the Low Pressure Auxiliary Fluid Spray" (in French), *Romanian Journal of Technical Sciences*, Electricity and Power Series, Vol. 22, No. 2, 1977, pp. 289–297.

[5] Cristea, E.D., "Concerning the Swirled Flows Produced by Annular Vane Swirlers, under Enclosed Conditions, with Application on Low Pressure Auxiliary Fluid Spray Burners" (in Romanian), Technical and Scientific Meeting, Institute of Scientific Research and Engineering for Power Equipment, Bucharest, 1983, pp. 136–151.

[6] Gosman, A.D., et al., *Heat and Mass Transfer in Recirculating Flows*, Academic Press, London, 1969, pp. 18–137.

[7] Richter, W., "Mathematical Model of the Industrial Flame (Fundamentals and Application on Axisymmetric Systems)" (in German), Ph.D. Thesis, Stuttgart Univ., London, 1978, pp. 52–196.

[8] Cristea, E.D. and Petcu, M. "Mathematical Modelling for NonReacting, Recirculating Flows, with Application on Complete Burning System" (in Romanian), Technical and Scientific Meeting, Institute of Scientific Research and Engineering for Power Equipment, Bucharest, 1983, pp. 152–161.

[9] Cristea, E.D., "A Contribution to Research on Auxiliary Fluid Spray Burners for Industrial Furnaces" (in Romanian), Ph.D. Thesis, "Traian Vuia" Polytechnical Institute of Timisoara, Romania, 1984, pp. 16–87.

[10] Chigier, N.A. and Béer, J.M., "Velocity and Static Pressure Distributions in Swirling Air Jets Issuing from Annular and Divergent Nozzles," *Journal of Basic Engineering*, Vol. 86, Dec. 1964, pp. 788–798.

[11] Beltagui, S.A. and Macallum, H.R.L., "Aerodynamics of Vane-Swirled Flames in Furnace"; "The Modelling of Vane-Swirled Flames in Furnaces," *Journal of the Institute of Fuel*, Vol. 49, No. 401, Dec. 1976, pp. 183–200.